

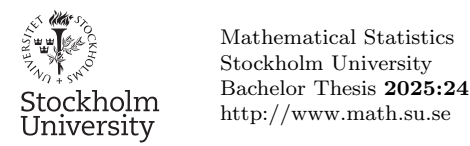
Timing is Everything: Comparing When and Whom to Vaccinate in Risk-Stratified Network Epidemics

Albin Ceder

Kandidatuppsats 2025:24 Matematisk statistik September 2025

www.math.su.se

Matematisk statistik Matematiska institutionen Stockholms universitet 106 91 Stockholm



# Timing is Everything: Comparing When and Whom to Vaccinate in Risk-Stratified Network Epidemics

Albin Ceder\*

September 2025

#### Abstract

We investigate epidemic dynamics and mitigation strategies in synthetic populations using the inhomogeneous SIRVD (iSIRVD) model on small-world networks. In our framework, individuals are divided into high- and low-risk groups with distinct probabilities of mortality upon infection. We implement pre-epidemic ("pulse") vaccination strategies, comparing random allocation to targeted vaccination of high-risk individuals. Simulations analyze how these strategies affect total mortality, considering varying vaccine coverage levels and intervention timing. Our results demonstrate that prioritizing high-risk individuals for vaccination consistently reduces epidemic mortality more effectively than random allocation, especially when vaccine resources are limited. These findings highlight the importance of risk-based mitigation measures in structured populations and illustrate the policy advantages of targeting vulnerable groups in public health interventions.

<sup>\*</sup>Postal address: Mathematical Statistics, Stockholm University, SE-106 91, Sweden. E-mail: albin@cedercentral.com. Supervisor: Maria Deijfen.

# Contents

1	Intr	roduction	3
	1.1	Background	3
	1.2	Aim	4
	1.3	Delimitations	4
	1.4	Outline	5
2	The	eory	6
	2.1	Compartmental Epidemic Models	6
		2.1.1 Graph-based SIRVD Model (Discrete Time)	6
		2.1.2 Risk Group Stratification: The iSIRVD Model	8
	2.2	Network Models for Epidemics	10
		2.2.1 The Watts-Strogatz Small-World Model	10
	2.3	Vaccination and Risk-Based Mitigation Strategies	12
		2.3.1 The Basic Reproduction Number and Herd Immunity	
		Threshold	12
		2.3.2 Risk-Based and Network-Aware Vaccination Strategies	12
		2.3.3 Policy Implications and Limitations	13
3	Me	thods and Implementation	14
	3.1	Epidemic Model	14
	3.2	Risk Group Assignment	14
	3.3	Network Construction	15
	3.4	Vaccination Strategies	15
	3.5	Simulation Protocol	16
	3.6	Simulation Parameters	17
	3.7	Software and Computational Tools	19
4	Exp	perimental Design and Analysis	20
	4.1	Overview	20
	4.2	Research Questions and Hypotheses	20
	13	Sconario Construction	21

	4.4	Performance Metrics	21
	4.5	Analytical Methods	22
5	Res	ults	23
	5.1	Effect of Network Rewiring Probability	23
	5.2	Vaccination Outcomes by Strategy, Timing, and Risk Group .	24
		5.2.1 Population-Level Effects	24
		5.2.2 Risk-Stratified Outcomes and Trade-offs	24
6	Disc	cussion	26
	6.1	Risk Stratification as the Key Mechanism	26
	6.2	Trade-offs and Implementation Challenges	26
	6.3	Timing Considerations	27
	6.4	Effect of Network Rewiring Probability	27
	6.5	Policy Implications	27
	6.6	Limitations	27
	6.7	Future Work	28
	6.8	Conclusion	28
7	Ack	nowledgements	29
$\mathbf{A}$	Add	litional Figures and Tables	30
	A.1	Network Topology Robustness Analysis	30
В	Cod	le	32
	B.1	Computational Implementation	32
		B.1.1 Performance Metrics	32
		B 1.2 Code Availability	32

# Introduction

#### 1.1 Background

Infectious disease outbreaks remain a persistent threat to public health and highlight the importance of robust analytical tools for anticipating epidemic dynamics and evaluating interventions. Mathematical models play a central role in this task, enabling both researchers and policymakers to anticipate the progression of outbreaks and assess potential control strategies before implementation [1]. The traditional approach to modeling infectious diseases employs compartmental models, such as the susceptible-infectious-recovered (SIR) framework [2]. While such models have provided valuable insights into epidemic dynamics, they often assume homogeneous mixing, not reflecting the structured nature of real-world contact networks [3].

In reality, individuals are embedded in social and spatial networks that constrain and channel disease transmission. Epidemics in such structured populations can differ substantially from the predictions of well-mixed models [4]. Network-based epidemic models, where nodes represent individuals and edges represent potentially infectious contacts, address these structures and offer more realistic simulations of outbreaks. For instance, small-world networks—which combine high clustering with short average path lengths—have been shown to influence both the speed and extent of epidemic spread [5].

Incorporating network structure is also crucial for evaluating interventions such as vaccination. The effectiveness of these measures depends not just on coverage but also on the organization of contacts and the distribution of risk within the population [6]. Risk stratification—directing interventions toward those at greatest risk of severe outcomes—has become a central public health strategy, especially in the context of COVID-19 [7].

Building on these developments, the present study examines how risk-based vaccination strategies affect outbreak trajectories in structured networks, with a focus on the benefits of targeting high-risk individuals to reduce mortality.

#### 1.2 Aim

This thesis investigates how targeted and random pulse vaccination strategies—applied either before or during an epidemic—affect mortality and epidemic size in small-world networks, using an inhomogeneous SIRVD (iSIRVD) model. Particular attention is given to how the timing of vaccination interventions and the allocation of vaccine doses between high- and low-risk groups shape these outcomes.

Previous research has leveraged network-based epidemic models, especially those incorporating small-world features, to identify how the structure of social contacts shapes disease dynamics [5, 8]. Recent studies emphasize improving vaccine strategy timing and targeting, including optimal control approaches that dynamically minimize epidemic impacts [9] and gametheoretic analyses of individual behaviors and collective outcomes [10].

Modern models increasingly incorporate complex network features or adaptive features, with some demonstrating that hybrid strategies—such as those based on network centrality or other heuristics—are particularly effective in large or heterogeneous populations [11]. Other approaches enhance model realism by considering factors like region-specific contact patterns and population mobility [12].

In addition to transmission modeling, researchers have considered behavioral responses such as vaccine hesitancy [13] and strategies for promoting equitable vaccine access [14].

Nonetheless, most prior work tends to analyze either timing or allocation strategies in isolation, often assuming a static network. Comprehensive studies systematically comparing both timing and allocation—particularly using iSIRVD frameworks with explicit risk groups on small-world networks—remain limited [7, 1]. This study seeks to address this gap.

#### 1.3 Delimitations

This research relies exclusively on simulations using synthetic small-world networks and fixed risk groups, without empirical infection or mobility data [5, 8]. Models of optimal control, game-theoretic frameworks, behavioral re-

sponses, and equity-focused delivery are not implemented [9, 10, 14]. Additional interventions such as quarantine or other adaptive policies are also beyond the study's scope. Accordingly, results offer qualitative insights rather than precise forecasts for policy.

#### 1.4 Outline

The remainder of this thesis is organized as follows. Chapter 2 reviews the theoretical foundations of epidemic modeling, including compartmental and network-based frameworks, with particular emphasis on the SIRVD model and the Watts-Strogatz small-world network structure. Chapter 3 describes the methodological approach, detailing the construction of risk-stratified populations, network generation, vaccination strategies, and the simulation protocol. Chapter 4 presents the experimental design, including the formulation of research questions and hypothesis testing procedures. The results of these simulations are displayed in Chapter 5, focusing on the comparative effectiveness of targeted and random vaccination strategies under various scenarios. Chapter 6 discusses the main findings in the context of existing literature, evaluates the practical implications and potential limitations of the study, and outlines directions for future research. The thesis concludes with acknowledgements, as well as supplementary material and code provided in the appendices.

# Theory

#### 2.1 Compartmental Epidemic Models

Compartmental models are a foundational tool in infectious disease epidemiology [1]. These frameworks describe how individuals in a population move among mutually exclusive health states over time. To analyze intervention strategies and risk heterogeneity, we extend the classical SIR model as described below.

#### 2.1.1 Graph-based SIRVD Model (Discrete Time)

In this study, the SIRVD model is formulated on a contact network, represented by an undirected graph G = (V, E). Each node in V corresponds to an individual, and edges in E represent potential transmission routes (i.e., close-contact links).

The population is partitioned into five compartments: susceptible (S), infectious (I), recovered (R), vaccinated (V), and deceased (D). The size of each compartment evolves in discrete time steps (t), with transitions governed by the following probabilistic rules:

- At each timestep, every susceptible individual examines each network neighbor. For each infectious neighbor, a transmission event occurs independently with probability  $\beta$ . That is, a susceptible becomes infected with probability  $1-(1-\beta)^{k_I}$ , where  $k_I$  is the number of infectious neighbors.
- Susceptible individuals may also be vaccinated with probability  $\nu$ . In standard compartmental models, vaccination typically occurs continu-

ously, with a proportion of susceptible individuals vaccinated at each timestep.  $^{1}$ 

• Infectious individuals recover with probability  $\gamma$ , or die due to disease with probability  $\mu$ ; otherwise, they remain infectious. The sum  $\gamma + \mu$  cannot exceed 1, since it represents the total probability of leaving the infectious state per timestep.

The underlying contact network G is generated using a small-world algorithm; see Section 2.2.1 for details.

Vaccinated individuals are assumed to acquire complete and lasting immunity throughout the simulation.

$$S_{t+1} = S_t - \text{new infections}_t - \text{new vaccinations}_t$$

$$I_{t+1} = I_t + \text{new infections}_t - \text{new recoveries}_t - \text{new deaths}_t$$

$$R_{t+1} = R_t + \text{new recoveries}_t$$

$$V_{t+1} = V_t + \text{new vaccinations}_t$$

$$D_{t+1} = D_t + \text{new deaths}_t$$
(2.1)

Table 2.1: Variables and parameters for the discrete-time SIRVD model.

Symbol	Description
$S_t$	Number of susceptible individuals at time $t$
$I_t$	Number of infectious individuals at time $t$
$R_t$	Number of recovered individuals at time $t$
$V_t$	Number of vaccinated individuals at time $t$
$D_t$	Number of deceased individuals at time $t$
$\beta$	Probability of infection per susceptible per step
$\nu$	Probability of vaccination per susceptible per step
$\gamma$	Probability of recovery per infectious per step
$\mu$	Probability of disease-induced death per infectious per step

In standard compartmental models with homogeneous mixing (i.e., no underlying network), infection is modeled differently; here, we explicitly restrict infection events to occur along the edges of G only.

<sup>&</sup>lt;sup>1</sup>In this study, by contrast, vaccination is implemented as a one-time ("pulse") event, rather than a possibility at each timestep. See Chapter 3.4 for implementation details.

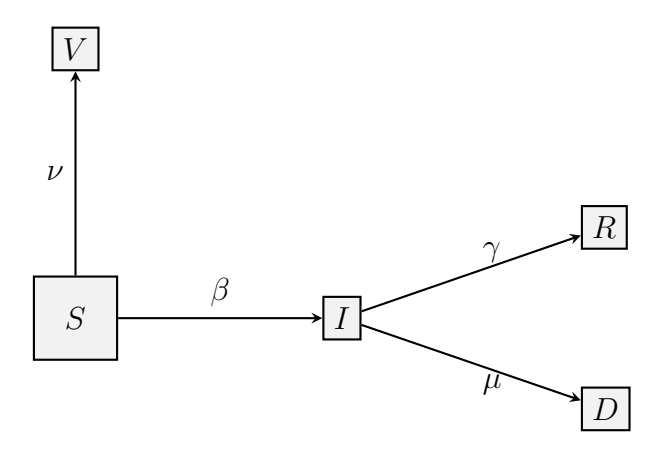


Figure 2.1: Flowchart of the discrete-time SIRVD model. Symbols: S = Susceptible, I = Infectious, R = Recovered, V = Vaccinated, D = Deceased. Transitions are governed by the per-step probabilities in Table 2.1.

#### 2.1.2 Risk Group Stratification: The iSIRVD Model

To represent differing disease risks, the population is stratified into high-risk and low-risk groups, giving the inhomogeneous SIRVD (iSIRVD) model [7]. Each node is randomly assigned to one risk group  $(g \in \{HR, LR\})$  at initialization, and retains this classification.

For each group g, the five compartments  $(S_g, I_g, R_g, V_g, D_g)$  are tracked separately. Transition probabilities are identical across groups except for the disease-induced death probability  $\mu_g$ , which is greater for the high-risk group. For all groups, the constraint  $\gamma + \mu_g \leq 1$  applies.

All disease transmission steps continue to occur exclusively along edges in the underlying network.

Table 2.2: Additional notation and parameters for the iSIRVD model, with risk group stratification.

Symbol	Description
$g \\ S_g, I_g, R_g, V_g, D_g \\ \mu_g$	Risk group: HR (high risk) or LR (low risk) Compartment counts for risk group $g$ Disease-induced death probability for group $g$ per time step

This framework allows simulation of targeted vaccination interventions and group-differentiated health outcomes under network-based epidemic scenarios. For further mathematical specifics and implementation details, see Section 3.1.

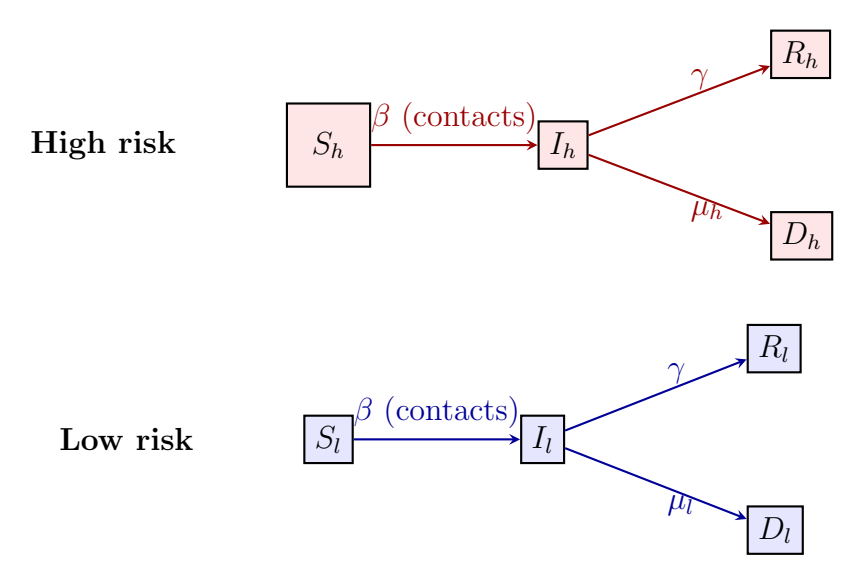


Figure 2.2: Flowchart of the discrete-time iSIRD model with high-risk  $(S_h, I_h, R_h, D_h)$  and low-risk  $(S_l, I_l, R_l, D_l)$  groups. Both groups share the same recovery probability  $(\gamma)$  but have group-specific mortality probabilities  $(\mu_h, \mu_l)$ .

#### Case Fatality Rate in the Discrete-Time SIRVD Model

It is important to clarify that the per-step, group-specific death probabilities  $(p_{\text{death,HR}}, p_{\text{death,LR}})$  set in the model dictate the likelihood of death given infection at each timestep, but do not correspond directly to the overall case fatality rate (CFR) observed over the course of the epidemic. In the discrete-time SIRVD dynamics, each infected individual either recovers (with probability  $p_{\text{rec}}$ ), dies (with probability  $p_{\text{death}}$ ), or remains infectious at each timestep. The probability that an individual ultimately dies from infection before recovering is given by:

$$CFR = \frac{p_{\text{death}}}{p_{\text{death}} + p_{\text{rec}}}$$
 (2.2)

This calculation applies independently to each risk group by substituting the corresponding death probability. For example, with  $p_{\text{death,HR}} = 0.04$  and  $p_{\text{rec,HR}} = 0.15$ , the high-risk group has a theoretical CFR of 0.210. For  $p_{\text{death,LR}} = 0.01$  and  $p_{\text{rec,LR}} = 0.15$ , the low-risk CFR is 0.0625.

Risk Group	$p_{\rm death}$	$p_{\rm rec}$	Theoretical CFR
High-Risk	0.04	0.15	0.210
Low-Risk	0.01	0.15	0.0625

Table 2.3: Input death and recovery probabilities with corresponding theoretical case fatality rate (CFR) in the iSIRVD framework.

Simulation results and reporting of CFR always refer to this emergent, model-based definition unless otherwise specified.

#### 2.2 Network Models for Epidemics

Traditional epidemic models often assume homogeneous mixing, where every individual is equally likely to contact any other. However, real populations exhibit complex patterns of social connections. Network-based models address this by representing individuals as graph nodes, with edges denoting potential transmission contacts [3, 4]. This approach captures heterogeneity in contact patterns, clustering, and community structure, all of which substantially influence disease dynamics compared to well-mixed models. NNetwork structure affects not only epidemic spread but also the impact of interventions such as vaccination and quarantining [8].

#### 2.2.1 The Watts-Strogatz Small-World Model

Let G = (V, E) be an undirected graph with N = |V| nodes, where N is the population size and K (even,  $K \ll N$ ) represents the number of neighbors each node connects to. The Watts-Strogatz (WS) model constructs G in two steps [5]:

1. Regular Ring Lattice: Place N nodes on a ring and connect each node  $i \in V$  to its K/2 nearest neighbors on each side:

$$E_0 = \{(i, j) \mid i \in V, 1 \le |i - j| \mod N \le K/2\}$$

This forms a K-regular lattice.

2. Random Rewiring: For each edge (i, j) with i < j in  $E_0$ , with probability p ( $0 \le p \le 1$ ), rewire the endpoint j to a new node  $l \ne i$ , selected uniformly at random from all nodes except i. If the chosen l would result in a self-loop (l = i) or would create a duplicate edge  $(i, l) \in E$ , a new l is selected uniformly at random, and this process is

repeated until a valid node is found. Each edge may be rewired only once.

By design, G is a simple, undirected graph with mean degree K for all p. The rewiring parameter p controls the transition from a regular lattice (p=0) with high clustering and long paths, to a random network (p=1) with low clustering and short average path length. It is only for small values of p that networks exhibit both high clustering and short average path lengths—defining the "small-world" regime—whereas clustering drops rapidly as p increases [5, 8].

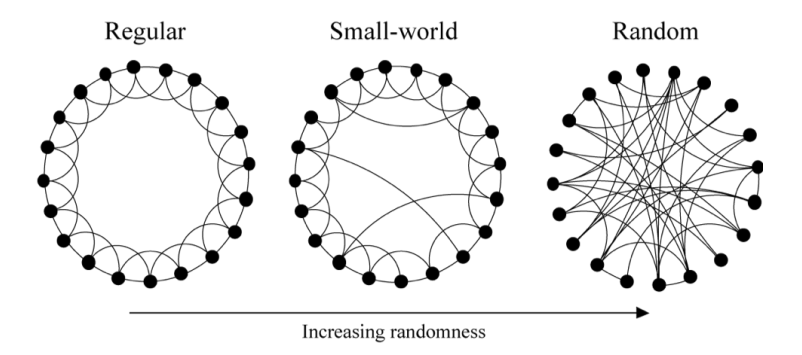


Figure 2.3: Transition from a regular lattice (p = 0) to small-world (0 and random <math>(p = 1) networks in the Watts-Strogatz model.

The parameter K determines each node's initial neighborhood size, while p sets network randomness. For intermediate p, clustering stays high but the mean shortest path length quickly drops to the random graph limit [5, 8]. The clustering coefficient for node i with degree  $k_i$  is:

$$C_i = \frac{2E_i}{k_i(k_i - 1)},\tag{2.3}$$

where  $E_i$  is the number of edges among *i*'s neighbors. The overall clustering coefficient C is the average over all nodes, while mean shortest path length L averages the minimal steps between pairs.

Small-world networks (low to intermediate p) include "shortcuts" that speed up spreading, similar to epidemic outbreaks. High clustering also changes local transmission and the effectiveness of certain interventions [5, 4, 8].

The WS model is used here for its relevance to social contact networks—balancing realism and computational efficiency. Still, it does not allow weighted or dynamic edges, heterogeneous degrees, or explicit community structure, which may limit its representation of real social systems [4, 8].

# 2.3 Vaccination and Risk-Based Mitigation Strategies

Vaccination is central to public health responses, substantially reducing cases and deaths due to infectious disease [7, 1]. By reducing the number of susceptible people (S), vaccination alters epidemic dynamics and lowers disease impact.

# 2.3.1 The Basic Reproduction Number and Herd Immunity Threshold

The basic reproduction number,  $R_0$ , is the expected number of secondary cases generated by a single infectious person in a fully susceptible population [1]. In compartmental models such as SIR,  $R_0$  determines whether an epidemic can take off  $(R_0 > 1)$  and is set by factors including transmission probability, contact rate, and infectious period.

Immunization lowers the effective reproduction number,  $R_{\rm eff}$ , by reducing the susceptible fraction. The critical vaccination coverage needed to halt sustained transmission in a well-mixed population—the so-called herd immunity threshold—is:

$$v_c = 1 - \frac{1}{R_0} \tag{2.4}$$

This result assumes random vaccination and homogeneous mixing, so that all individuals contribute equally to indirect protection [1]. In practice, population structure, heterogeneous risk, and imperfect vaccine effectiveness can cause real thresholds to differ from this prediction [8].

#### 2.3.2 Risk-Based and Network-Aware Vaccination Strategies

#### Risk Stratification and Targeted Vaccination

Populations show wide variation in infection risk, disease severity, contact patterns, and vaccine response [7, 1]. Risk-based vaccination gives priority to those at highest risk—such as the elderly or those with underlying conditions. Modeling results show that targeting these groups can greatly reduce severe cases and deaths, even at coverage below the classical herd immunity threshold [7]. In modeling studies, this is often represented by higher mortality or lower recovery rates for high-risk groups. Comparisons consistently find targeted strategies more effective than random allocation [7, 8].

#### **Network Effects and Structural Targeting**

Contact network structure strongly shapes epidemic spread and the impact of vaccination. In networks with heterogeneous degree distributions, highly connected individuals can play an outsized role in transmission. Vaccinating individuals based on their network position or structural properties can reduce epidemic size more efficiently than random allocation [6, 8].

By contrast, the small-world networks used in this study have a narrow degree distribution and lack highly connected hubs, but their high clustering and short average path lengths can still significantly affect epidemic dynamics and the outcomes of different vaccination strategies [5, 8].

#### 2.3.3 Policy Implications and Limitations

While targeted and network-informed vaccination strategies are generally more efficient and effective than non-targeted mass vaccination, practical and ethical challenges remain. These include identifying high-risk individuals fairly, protecting privacy, managing logistics, and ensuring public trust. Implementation may also be limited by data needs, organizational capacity, and vaccine acceptance. Nonetheless, both modeling and real-world evidence emphasize the importance of considering population structure and individual risk when designing epidemic policies [7, 8].

# Methods and Implementation

#### 3.1 Epidemic Model

We employ an inhomogeneous Susceptible-Infectious-Recovered-Vaccinated-Deceased (iSIRVD) model to simulate disease transmission on a dynamic network in discrete time, as detailed in Section 2.1. Each individual occupies a single compartment (S, I, R, V, or D) at each timestep. State transitions are applied synchronously according to group-specific transition probabilities.

Vaccination Implementation: Our model diverges from standard compartmental approaches by administering only a single discrete "pulse" vaccination event per simulation. This pulse occurs either pre-emptively at t=0 or reactively when the proportion of infectious individuals surpasses 10%, depending on the scenario. During the pulse, candidate individuals are randomly drawn from the combined pool of susceptible (S), infectious (I), and recovered (R) compartments until the intended coverage is achieved. Only candidates who are susceptible at the moment receive vaccination and acquire immunity; those drawn from I or R remain in their original states, resulting in a degree of vaccine wastage to reflect imperfect ascertainment.

All other disease state transitions—infection, recovery, and mortality—proceed as specified by the group-specific parameters described in Section 2.1.

#### 3.2 Risk Group Assignment

At initialization, each individual (node) is randomly assigned to one of two fixed risk groups:

• High-risk (HR, 35% of the population): per-timestep probability of death  $p_{\text{death,HR}} = 0.04$ .

• Low-risk (LR, 65%): per-timestep probability of death  $p_{\text{death,LR}} = 0.01$ .

Both groups share an identical per-timestep probability of recovery,  $p_{\text{rec}} = 0.15$ . All individuals also have a uniform per-contact transmission probability ( $\beta = 0.3$ ).

Because these transition probabilities apply at each discrete timestep, the overall probability that an infected individual ultimately dies (the case fatality rate, CFR) is not equal to the per-timestep death probability. Instead, for each group,

$$CFR_g = \frac{p_{\text{death},g}}{p_{\text{death},g} + p_{\text{rec}}}$$

yielding  $CFR_{HR} = 0.210$  and  $CFR_{LR} = 0.0625$  with the parameters above (see also Section 2.2).

These risk assignments determine the distribution of severity outcomes and inform targeted interventions in subsequent simulation steps.

#### 3.3 Network Construction

To capture realistic social contact patterns, we generate interaction networks using the Watts-Strogatz small-world model (see Section 2.2.1). By default, each network comprises N=1000 nodes, with mean node degree K=6 and rewiring probability p set to either 0.3 or 0.9 based on scenario. All networks are undirected, unweighted, and constructed without self-loops or multiple edges using fixed random seeds to ensure reproducibility. If a generated network is not fully connected, only the largest component is retained for analysis.

For each of the 500 simulation replicates per scenario, a fresh network topology and randomized risk group assignment are produced using unique seeds. This design guarantees statistical independence across replicates and ensures that outcome variability captures both stochastic epidemic dynamics and underlying network structure.

#### 3.4 Vaccination Strategies

This study systematically compares two strategies for allocating a fixed number of vaccine doses:

Parameter	Value(s)
Number of nodes $(N)$	1000
Mean degree $(K)$	6
Rewiring probability $(p)$	0.3,  0.9
Replicates per scenario	500

Table 3.1: Default parameters for Watts-Strogatz network generation in simulation experiments.

- Random Vaccination: Vaccine doses are allocated by randomly selecting eligible individuals from the entire living population until the desired coverage level is reached.
- Targeted Vaccination: High-risk individuals are prioritized for vaccination. If the coverage target exceeds the size of the high-risk group (35%), any remaining doses are distributed at random among low-risk individuals.

Scenarios vary by:

- Timing of Vaccination:
  - Start: Prior to introduction of infection (t=0)
  - Early: At the first time step when at least 10% of individuals are infectious
- Coverage Rate: 15%, 20%, or 25% of the population

Within each scenario, vaccination is implemented as a single "pulse" event per simulation, and candidates for vaccination are drawn from non-deceased individuals, regardless of current infection status, to model imperfect status ascertainment.

#### 3.5 Simulation Protocol

Each simulation replicate follows these procedural steps:

1. **Initialization:** Set scenario parameters (strategy, timing, and coverage). Generate the Watts-Strogatz contact network and assign each individual to a fixed risk group. Set all nodes to susceptible (S), except for a single randomly selected node that is set to infectious (I).

#### 2. Time Step Iteration:

- Vaccination: At either t=0 or when the early-vaccination threshold is reached (10% infected), implement a single vaccination pulse according to the assigned strategy. Randomly select vaccine recipients from the current non-deceased population until the coverage level is reached. Only susceptible individuals immediately benefit; individuals in I or R remain unchanged, modeling operational wastage.
- **Transmission:** For each infectious (I) node, attempt to infect all susceptible (S) neighbors with probability  $\beta$  per contact.
- **Progression:** For each I node, determine transition to recovered (R), deceased (D), or remain infectious, according to group-specific probabilities.
- Removal: Remove deceased individuals and associated edges.
- Synchronization: Update all individual states for the next time step.
- 3. Repeat until no infectious (I) individuals remain.

#### 3.6 Simulation Parameters

Unless stated otherwise, the following parameters are used:

Table 3.2: Default simulation parameters.

$\begin{array}{c ccccccccccccccccccccccccccccccccccc$	Parameter	Value / Sym-	Description
Recovery rate $\gamma = 0.15$ Probability of recovery per time step  Mortality rate, low risk $\mu_{LR} = 0.01$ Per-timestep death probability  Mortality rate, high risk $\mu_{HR} = 0.04$ Per-timestep death probability  Case fatality rate, low risk $\mu_{LR} = 0.062$ Actual mortality among infected  Case fatality rate, high risk $\mu_{LR} = 0.062$ Actual mortality among infected  Fraction high-risk $\mu_{LR} = 0.211$ Actual mortality among infected  Fraction high-risk $\mu_{LR} = 0.211$ Actual mortality among infected  Fraction high-risk $\mu_{LR} = 0.211$ Actual mortality among infected  Fraction high-risk $\mu_{LR} = 0.211$ Actual mortality among infected  Fraction high-risk $\mu_{LR} = 0.211$ Actual mortality among infected  Fraction high-risk $\mu_{LR} = 0.211$ Actual mortality among infected  Fraction high-risk $\mu_{LR} = 0.211$ Actual mortality among infected  Fraction high-risk $\mu_{LR} = 0.211$ Actual mortality among infected  Fraction high-risk $\mu_{LR} = 0.211$ Actual mortality among infected  Fraction high-risk $\mu_{LR} = 0.211$ Actual mortality among infected  Fraction high-risk $\mu_{LR} = 0.211$ Actual mortality among infected  Fraction high-risk $\mu_{LR} = 0.211$ Actual mortality among infected  Fraction high-risk $\mu_{LR} = 0.211$ Actual mortality among infected  Fraction high-risk group  Initial infectious cases $\mu_{LR} = 0.211$ Actual mortality among infected  Fraction high-risk group  Initial infectious cases $\mu_{LR} = 0.211$ Actual mortality among infected  Fraction high-risk group  Initial infectious cases $\mu_{LR} = 0.211$ Actual mortality among infected  Fraction high-risk group  Initial infectious cases $\mu_{LR} = 0.211$ Actual mortality among infected  Fraction high-risk group  Initial infectious cases $\mu_{LR} = 0.211$ Actual mortality among infected  Fraction high-risk group  Initial infectious cases $\mu_{LR} = 0.211$ Actual mortality among infected  Fraction high-risk group among infected  Initial infectious cases $\mu_{LR} = 0.211$ Actual mortality among infected  Initial infectious cases $\mu_{LR} = 0.211$ Actual mortali		, •	2 osoripulon
$\begin{array}{llllllllllllllllllllllllllllllllllll$	Transmission probability per contact	$\beta = 0.3$	Per-contact transmis-
$ \begin{array}{cccccccccccccccccccccccccccccccccccc$			sion risk
$\begin{array}{llllllllllllllllllllllllllllllllllll$	Recovery rate	$\gamma = 0.15$	Probability of recov-
$ \begin{array}{cccccccccccccccccccccccccccccccccccc$			v
Mortality rate, high risk $\mu_{\rm HR} = 0.04$ Per-timestep death probability  Case fatality rate, low risk CFR <sub>LR</sub> = 0.062 Actual mortality among infected  Case fatality rate, high risk CFR <sub>HR</sub> = 0.211 Actual mortality among infected  Fraction high-risk 0.35 Population share in high-risk group  Initial infectious cases $n_0 = 1$ Seed infections at $t = 0$ Network size $N = 1000$ Number of individuals  Mean node degree $K = 6$ Average contacts per	Mortality rate, low risk	$\mu_{\rm LR} = 0.01$	•
Case fatality rate, low risk $CFR_{LR} = 0.062$ Actual mortality among infected Case fatality rate, high risk $CFR_{HR} = 0.211$ Actual mortality among infected Fraction high-risk $0.35$ Population share in high-risk group Initial infectious cases $n_0 = 1$ Seed infections at $t = 0$ Network size $N = 1000$ Number of individuals Mean node degree $K = 6$ Average contacts per			2
$ \begin{array}{cccccccccccccccccccccccccccccccccccc$	Mortality rate, high risk	$\mu_{\rm HR} = 0.04$	•
$ \begin{array}{cccccccccccccccccccccccccccccccccccc$			- v
$ \begin{array}{cccccccccccccccccccccccccccccccccccc$	Case fatality rate, low risk	$\mathbf{CFR}_{\mathrm{LR}} = 0.062$	
Fraction high-risk $0.35$ Population share in high-risk group  Initial infectious cases $n_0=1$ Seed infections at $t=0$ Network size $N=1000$ Number of individuals Mean node degree $K=6$ Average contacts per		CED 0.011	_
Fraction high-risk 0.35 Population share in high-risk group Initial infectious cases $n_0=1$ Seed infections at $t=0$ Network size $N=1000$ Number of individuals Mean node degree $K=6$ Average contacts per	Case fatality rate, high risk	$\mathbf{CFR}_{\mathrm{HR}} = 0.211$	·
Initial infectious cases $n_0 = 1$ Seed infections at $t = 0$ Network size $N = 1000$ Number of individuals Mean node degree $K = 6$ Average contacts per		0.95	9
Initial infectious cases $n_0 = 1$ Seed infections at $t = 0$ Network size $N = 1000$ Number of individuals Mean node degree $K = 6$ Average contacts per	Fraction nign-risk	0.35	_
Network size $N=1000$ Number of individuals Mean node degree $K=6$ Average contacts per	Initial infactions codes	m — 1	0 0 1
Network size $N = 1000$ Number of individuals Mean node degree $K = 6$ Average contacts per	mittai miectious cases	$n_0 = 1$	
Mean node degree $K=6$ Average contacts per	Network size	N = 1000	O .
0 1			
node	Wear hode degree	H = 0	_
Rewiring probability $p \in \{0.3, 0.9\}$ Watts-Strogatz	Rewiring probability	$n \in \{0, 3, 0, 9\}$	
"small-worldness"	rewining probability	$p \in \{0.0, 0.0\}$	9
Vaccination coverage [0.15, 0.20, 0.25] Fraction immunized	Vaccination coverage	[0.15, 0.20, 0.25]	
per strategy		[0.20, 0.20, 0.20]	
Early vaccination threshold 0.10 Infection threshold for	Early vaccination threshold	0.10	2 00
early timing	V		
Simulations per scenario 500 Replicates for averag-	Simulations per scenario	500	v C
ing/stats	•		

#### Parameter Selection and Justification

The simulation parameters (Table 3.2) are chosen to balance computational tractability, epidemiological plausibility, and the ability to robustly detect differences between intervention strategies. Network parameters—the population size (N=1000) and mean degree (K=6)—are selected to provide a sufficiently large and interconnected model population, while keeping simulations manageable. The rewiring probabilities  $(p \in \{0.3, 0.9\})$  allow comparison of clustered small-world and effectively random network structures,

following established modeling frameworks [5].

Epidemic parameters, including the per-contact transmission probability ( $\beta=0.3$ ) and per-timestep recovery probability ( $p_{\rm rec}=0.15$ ), yield moderately sized outbreaks without trivial (extinction) or explosive (saturation) dynamics.

The model's case fatality rates for low-risk (6.2%) and high-risk (21.1%) groups, determined from the combination of per-timestep death and recovery probabilities (see Section 2.2), are set higher than typical for common diseases. This deliberate choice enhances the contrast between vaccination strategies, ensuring detectable effects in a simulated population of N=1000 individuals and a realistic number of epidemic events. The model thus represents a severe pandemic setting, where intervention strategy is crucial for public health outcomes.

Vaccination coverage rates between 15-25% reflect the limited supply scenarios often encountered during the first phases of a pandemic. Performing 500 independent simulation replicates per scenario ensures stable statistical estimates, while accounting for the inherent stochasticity of network-based disease transmission.

Overall, this parameterization is designed to maximize the ability to distinguish intervention effects under operationally realistic constraints, with a primary focus on comparing the relative performance of different vaccination strategies.

#### 3.7 Software and Computational Tools

Simulations are implemented in Python 3.10 using the following libraries:

- NetworkX for network generation and manipulation
- NumPy for numerical operations and random sampling
- Pandas and Matplotlib for data storage, management, and visualization

All random number generators use fixed seeds for reproducibility.

# Experimental Design and Analysis

#### 4.1 Overview

This chapter details the comparative framework for evaluating how different vaccination strategies influence epidemic outcomes on small-world networks. The design systematically explores the effects of allocation approach, timing, coverage, and network structure through structured simulation scenarios.

#### 4.2 Research Questions and Hypotheses

The study addresses two central research questions:

- 1. Does prioritizing high-risk individuals for vaccination reduce overall mortality more effectively than random vaccination?
- 2. How does vaccination timing—pre-outbreak (start) versus reactive (early, after 10% infection prevalence)—affect the relative effectiveness of each strategy?

The corresponding hypotheses are:

- **H1:** Targeted (high-risk) vaccination reduces total mortality more effectively than random allocation, while potentially increasing mortality among unvaccinated low-risk individuals.
- **H2:** Pre-emptive vaccination yields greater reductions in mortality than early reactive vaccination, with the magnitude of this effect dependent on network structure and coverage level.

#### 4.3 Scenario Construction

Simulation scenarios are fully defined by four parameters: network rewiring probability (p), vaccination strategy, coverage rate, and timing of vaccine deployment. The parameter grid is shown in Table 4.1. Each combination (for a total of  $2 \times 3 \times 2 \times 2 = 24$  scenarios) is replicated 500 times, using independently generated networks and randomized risk group assignments, to ensure robust and representative results.

Table 4.1: Parameter combinations for simulation scenarios

Parameter	Values
Network rewiring probability	0.3, 0.9
Vaccination coverage rate	15%, $20%$ , $25%$
Vaccination strategy	Random, Targeted
Vaccination timing	Start (pre-outbreak), Early (10% infected)

These scenarios support systematic evaluation of:

• Strategy effectiveness: Random vs targeted vaccination

• Coverage response: Effects across increasing coverage rates

• Timing sensitivity: Start vs early vaccination

• Network dependency: Influence of rewiring probability

#### 4.4 Performance Metrics

To directly address the research questions, the following outcome measures are computed for each scenario (see Table 4.2 for details):

- Total epidemic mortality (overall deaths)
- High-risk and low-risk group mortality

All metrics are reported stratified by vaccination strategy, timing, coverage, and network structure. Other epidemiological outcomes—such as attack rate or peak prevalence—are not included as primary endpoints; metrics are selected for direct alignment with the study hypotheses.

Metric	Notation	Description
High-risk mortality	$M_{HR} = \frac{D_{HR}}{N_{HR}}$	Proportion of high-risk individuals who
	- · H K	die during the simulation
Low-risk mortality	$M_{LR} = \frac{D_{LR}}{N_{LR}}$	Proportion of low-risk individuals who
	EII	die during the simulation
Total mortality	$M_{total} = \frac{D_{HR} + D_{LR}}{N_{total}}$	Proportion of all individuals who die
	1 vtotal	during the simulation

Table 4.2: Performance metrics used to evaluate vaccination strategies and timing across scenarios.

## 4.5 Analytical Methods

For each scenario, simulation outputs are summarized by means and, where relevant, 95% confidence intervals or selected percentiles across 500 replicates. No formal inferential (statistical) hypothesis tests are used, as all principal comparisons are within a closed set of exhaustively simulated scenarios, rather than population-level inference.

# Results

### 5.1 Effect of Network Rewiring Probability

Preliminary analysis confirmed that epidemic outcomes are robust to network topology within the examined parameter range. Comparisons between small-world (p=0.3) and random-like (p=0.9) networks showed virtually identical mortality and epidemic size across all vaccination scenarios (see Appendix A.1). All subsequent analyses therefore use p=0.3 as the default configuration.

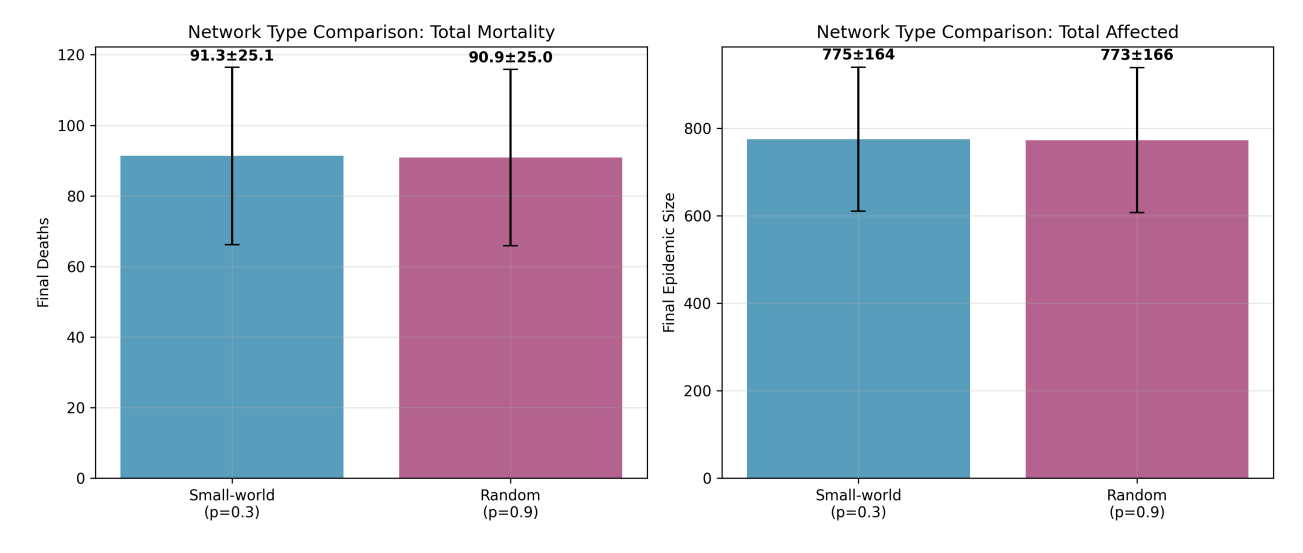


Figure 5.1: Detailed comparison of total mortality and total infected across network topologies. Error bars show standard deviations over 500 replicates.

# 5.2 Vaccination Outcomes by Strategy, Timing, and Risk Group

This section presents results using all mortality metrics defined in Table 4.2: absolute and proportional mortality for both high- and low-risk groups, as well as total mortality.

#### 5.2.1 Population-Level Effects

Targeted vaccination strategies consistently reduced mean total mortality  $(M_{\text{total}})$  compared to random allocation at all coverage levels (Table 5.1). For example, at 15% coverage, targeted-start vaccination yielded an average of  $M_{\text{total}} = 93.6$  deaths, a 20.1% reduction relative to random-early (117.2 deaths).

Expressed as a proportion of the total population  $(N_{\text{total}})$ , this corresponds to  $N_{\text{total}} = 0.094$  for targeted-start versus 0.117 for random-early vaccination (assuming N = 1000). Both  $M_{\text{total}}$  and  $N_{\text{total}}$  improved further at higher coverage, reaching  $M_{\text{total}} = 65.0$  and  $N_{\text{total}} = 0.065$  at 25% coverage under targeted-start (vs.  $M_{\text{total}} = 104.2$ ,  $N_{\text{total}} = 0.104$  for random-early; a 37.6% improvement).

Vaccination timing also impacted outcomes: start-of-epidemic administration led to lower mortality than early reactive vaccination for both total deaths  $(M_{\text{total}})$  and proportion  $(N_{\text{total}})$ . The effect was more pronounced for targeted than random strategies.

#### 5.2.2 Risk-Stratified Outcomes and Trade-offs

Outcomes for high- and low-risk groups are summarized in both absolute  $(M_{\rm HR}, M_{\rm LR})$  and proportional terms  $(N_{\rm HR}, N_{\rm LR})$  in Table 5.1.

Targeted allocation substantially reduced both absolute and proportional mortality among high-risk individuals: at 15% coverage, mean high-risk deaths were  $M_{\rm HR}=51.9~(N_{\rm HR}=0.52)$  for targeted-start, versus  $M_{\rm HR}=80.2~(N_{\rm HR}=0.80)$  for random-early. At 25% coverage, targeted-start resulted in  $M_{\rm HR}=24.7~(N_{\rm HR}=0.25)$ , reducing both the number and risk-group-specific proportion of high-risk deaths by over 65% compared to random-early.

By contrast, targeted vaccination led to a modest increase in low-risk mortality:  $M_{\rm LR} = 41.7 \, (N_{\rm LR} = 0.042)$  for targeted-start, compared to  $M_{\rm LR} = 37.0 \, (N_{\rm LR} = 0.037)$  for random-early at 15% coverage; the increases were outweighed by the reduction in high-risk mortality.

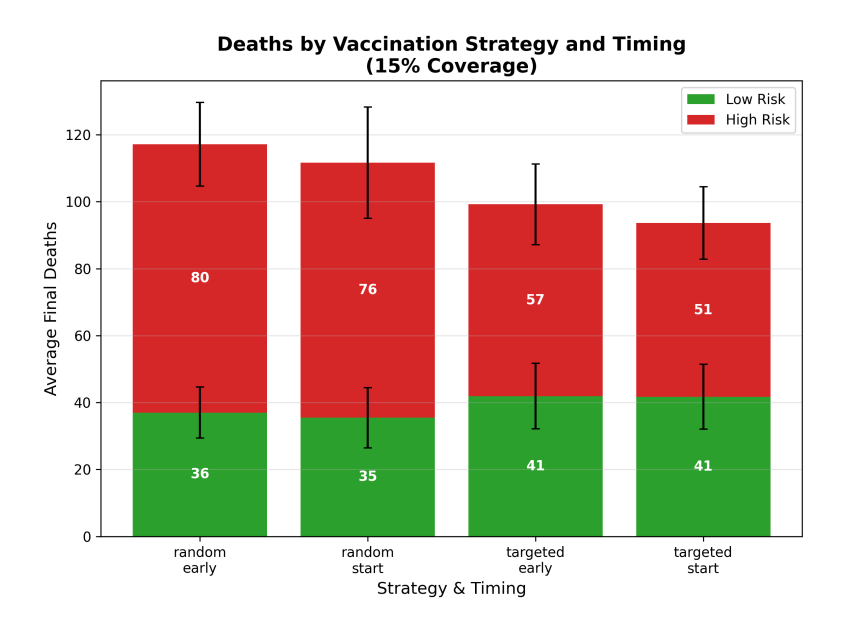


Figure 5.2: Total mortality metrics  $(M_{\text{total}}, N_{\text{total}})$  by vaccination strategy and timing at 15% coverage.

Table 5.1: Absolute (M) and proportional (N) mortality by risk group and strategy. Proportions are relative to group or total size.

Strategy	$M_{ m HR}$	$N_{ m HR}$	$M_{ m LR}$	$N_{ m LR}$	$M_{ m total}$	$N_{ m total}$
Targeted-start, 15% Random-early, 15%						

# Discussion

#### 6.1 Risk Stratification as the Key Mechanism

Our simulations indicate that prioritizing high-risk individuals for vaccination yields the greatest reduction in mortality per vaccine dose, consistent with established public health principles [7]. In networks with p=0.3, targeted vaccination reduced mean total deaths by 18.6% at 15% coverage (87.8 vs 112.6), 29% at 20% coverage (74.7 vs 105.3), and 39% at 25% coverage (61.2 vs 100.4), compared to random vaccination. The benefit arose almost entirely from a reduction in high-risk mortality: at 25% coverage, targeted allocation reduced high-risk deaths by 66% (23.5 vs 69.0). However, targeted allocation was associated with a 16–20% increase in low-risk deaths (e.g., 37.7 vs 31.5 at 25% coverage), a trade-off decisively outweighed by the much larger reduction among high-risk groups. These results underscore the importance of focusing limited vaccination resources on populations most vulnerable to severe outcomes.

#### 6.2 Trade-offs and Implementation Challenges

While risk-based targeting offers clear epidemiological advantages, practical implementation faces challenges. Our modeling assumes perfect identification and delivery to high-risk individuals, whereas misclassification, incomplete data, or logistical constraints could erode real-world effectiveness. Although targeted schemes may lead to modest increases in mortality among low-risk individuals (as noted above), these are far outweighed by substantial reductions among high-risk groups, making targeted allocation more effective at minimizing overall deaths. Random allocation, though logistically simpler, is considerably less efficient at reducing mortality.

#### 6.3 Timing Considerations

The timing of vaccination—whether before epidemic onset or reactive during outbreak growth—produced only minor differences in total mortality within the explored parameter space. For instance, shifting from start-of-epidemic to reactive timing (at 15% coverage) reduced total deaths by up to 4.6 (random strategy) and up to 9.8 (targeted strategy), compared to the total difference of 24.8 fewer deaths between targeted and random strategies. This suggests that, for epidemics with characteristics similar to those modeled here, accurately targeting high-risk groups is substantially more impactful than acceleration of rollout.

#### 6.4 Effect of Network Rewiring Probability

Empirical results demonstrated that epidemic outcomes—including total mortality and final epidemic size—were virtually identical across Watts-Strogatz networks with p=0.3 (small-world) and p=0.9 (random-like), for all vaccination scenarios studied. Therefore, outcome sensitivity to network topology was minimal within the examined parameter range, justifying p=0.3 as the standard in all further analyses [5].

#### 6.5 Policy Implications

These results highlight the importance of epidemic preparedness plans that support robust systems for risk identification and flexible strategies to overcome logistical challenges [7]. As vaccine availability expands, phased approaches can broaden eligibility to additional groups, but initial efforts should prioritize those populations likely to benefit most, based on risk profiles. The minimal effect of timing in this model underlines the importance of careful prioritization over rollout speed.

#### 6.6 Limitations

These findings should be interpreted in light of several limitations. The model assumes perfect and instantaneous vaccine protection, two discrete risk groups, and a pulse vaccination approach. In practice, vaccine effectiveness varies, protection may be delayed, and risk is typically continuous [1]. The modeled population structure employs a simplified Watts-Strogatz network; control simulations varying the rewiring parameter (p = 0.3 and p = 0.9)

showed no significant effect on total mortality in this context. Further, dynamic processes—such as virus evolution, seasonality, behavioral adaptation, or waning immunity—were not included, though each could substantially alter real-world outcomes [6].

#### 6.7 Future Work

To improve real-world relevance, future studies should incorporate imperfect risk identification, variable or delayed vaccine immunity, and ongoing vaccination strategies. Considering more complex population structures, such as variable mixing between age groups or communities, will enhance generalizability [7, 6]. Integrating factors like behavioral response, vaccine hesitancy, and economic evaluation could further inform actionable policy. Additionally, examining scenarios where timing and network effects are more pronounced, and validating models against empirical or highly resolved synthetic data, would extend applicability and support practical epidemic planning.

#### 6.8 Conclusion

In summary, this study demonstrates that risk-based vaccine allocation can substantially reduce mortality compared to random distribution, reinforcing the value of prioritizing vulnerable populations when vaccine resources are limited. While vaccine timing and network structure had comparatively minor effects in our model, further research should delineate the conditions under which this generalizes to other pathogens and real-world complexities. Incorporating nuanced risk assessment, logistical challenges, and dynamic epidemic factors will be critical for translating these findings into public health practice.

# Acknowledgements

I would like to acknowledge and give thanks to my supervisor, Maria Deijfen, for thorough feedback and guidance on how to make the formulation and thesis more concrete.

#### AI Assistance Statement

Portions of this thesis were refined using AI-based writing tools, which were employed exclusively for language editing, clarification of syntax, assistance with LaTeX formatting, code debugging, and the generation of structural outlines and skeletons for code and text segments. No AI tool was used to generate research hypotheses, analytical logic, simulation design, or to select methodological frameworks. All core analyses, theoretical developments, and conclusions presented in this work are original and my own, or otherwise appropriately referenced. Visualization layout suggestions made by AI were adopted solely for improving the clarity of data presentation, with all substantive figure content generated by me.

# Appendix A

# Additional Figures and Tables

## A.1 Network Topology Robustness Analysis

This section provides detailed validation that our results are robust to network structure variations.

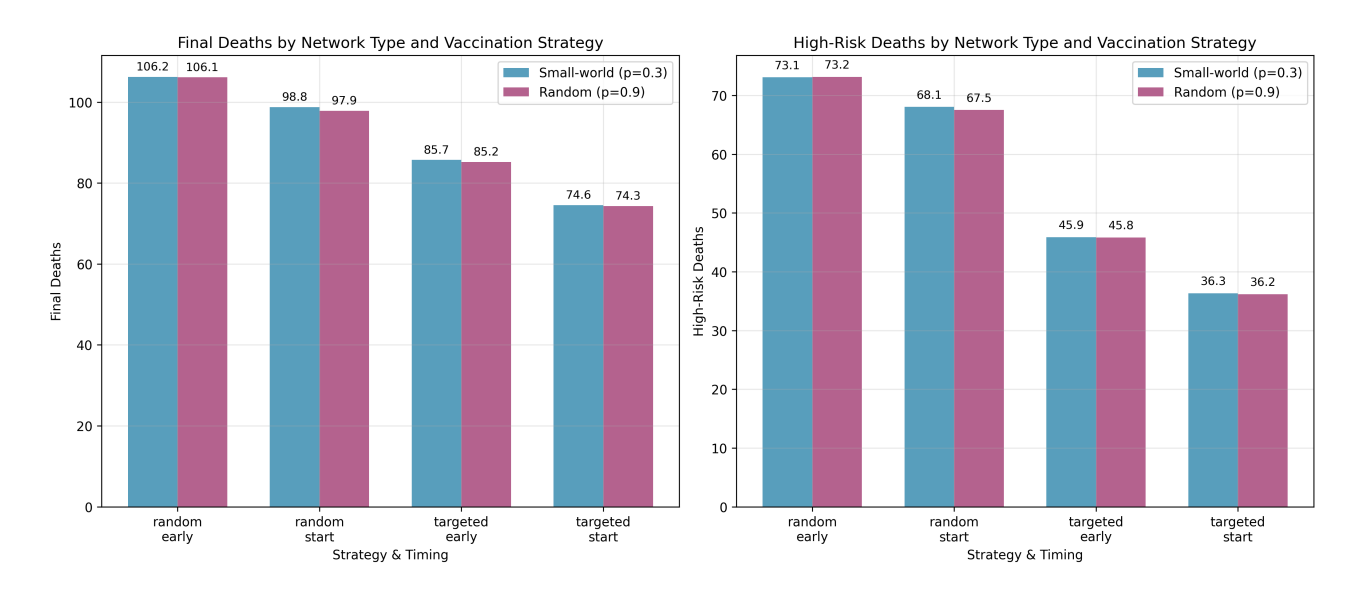


Figure A.1: Final deaths by vaccination strategy and timing across network topologies. Results demonstrate robustness to network structure.

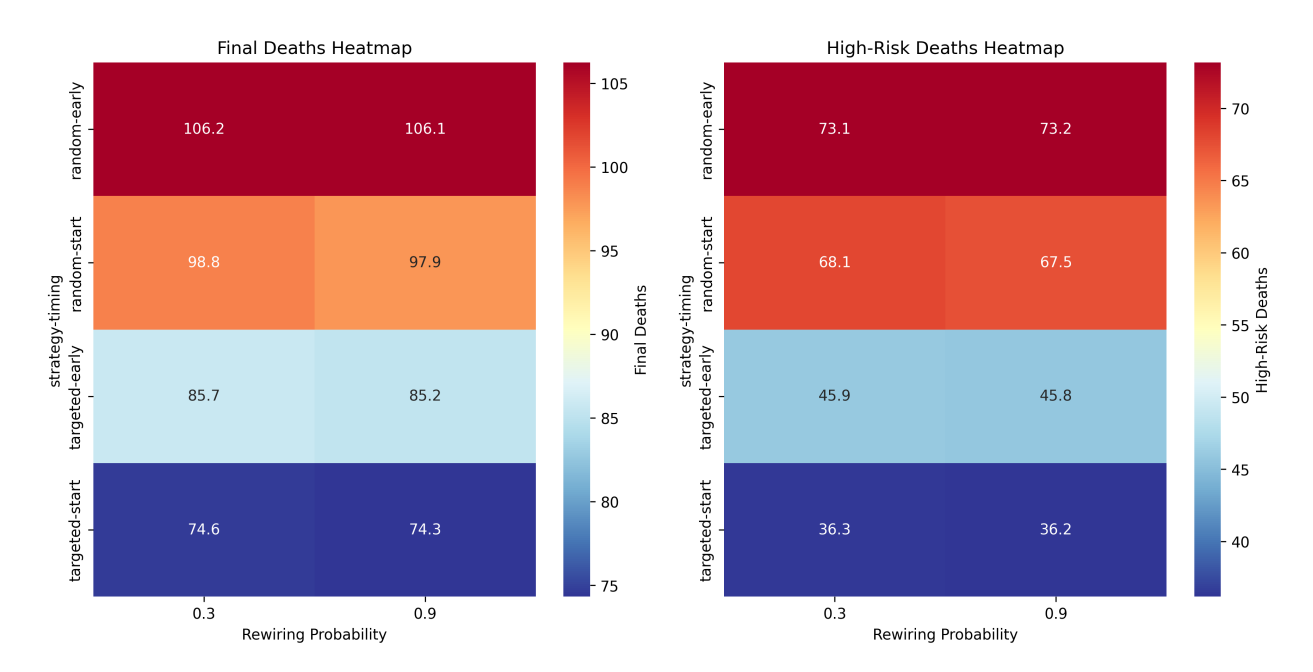


Figure A.2: Comprehensive heatmap analysis showing final deaths and highrisk deaths by strategy-timing combination across network types. Darker shading indicates higher death counts.

The consistency across topologies validates that our vaccination strategy conclusions are not dependent on specific network structural assumptions.

# Appendix B

# Code

### **B.1** Computational Implementation

#### **B.1.1** Performance Metrics

• Peak memory usage: 23.5 MB

• Total compute time: 0.02 hours for 6000 simulations

• Average time per simulation: 0.012 seconds

#### B.1.2 Code Availability

Repository: https://github.com/AlbinAbsint/Bachelor\_Thesis Key modules:

- epidemic\_model.py: SIRVD dynamics implementation
- simulation.py: Epidemic simulation
- network.py: Watts-Strogatz network generator
- visualize\_plots.py: Results analysis and plotting

All results are fully reproducible using documented random seeds and parameter configurations.

# **Bibliography**

- [1] Roy M. Anderson and Robert M. May. *Infectious Diseases of Humans: Dynamics and Control.* Oxford University Press, 1991.
- [2] William O. Kermack and Anderson G. McKendrick. A contribution to the mathematical theory of epidemics. *Proceedings of the Royal Society* of London. Series A, 115(772):700–721, 1927.
- [3] Matt J. Keeling and Ken TD Eames. Networks and epidemic models. Journal of the Royal Society Interface, 2(4):295–307, 2005.
- [4] Mark EJ Newman. *Networks: An Introduction*. Oxford University Press, 2010.
- [5] Duncan J Watts and Steven H Strogatz. Collective dynamics of 'smallworld' networks. *Nature*, 393(6684):440–442, 1998.
- [6] Marcel Salathé and James H. Jones. Dynamics and control of diseases in networks with community structure. PLoS Computational Biology, 6(4):e1000736, 2010.
- [7] Kate M Bubar, Katelyn Reinholt, Stephen M Kissler, et al. Model-informed covid-19 vaccine prioritization strategies by age and serostatus. *Science*, 371(6532):916–921, 2021.
- [8] Romualdo Pastor-Satorras, Claudio Castellano, Piet Van Mieghem, and Alessandro Vespignani. Epidemic processes in complex networks. *Reviews of Modern Physics*, 87(3):925–979, 2015.
- [9] Samir Riouali et al. Optimal control strategies for seqirs pandemic model using pontryagin's maximum principle. *Mathematical Biosciences and Engineering*, 20(7):12066–12093, 2023.
- [10] Paula Doutor et al. Optimal vaccination strategies: A game theory approach for pandemic control. *Journal of Theoretical Biology*, 578:111686, 2024.

- [11] Ricardo J. Sánchez-García, Peter G. Fennell, Shai Norris, James P. Gleeson, and Sergey Melnik. A comparison of node vaccination strategies to halt sir epidemic spreading in real-world complex networks. *Scientific Reports*, 12(1):21355, 2022.
- [12] Matteo Chinazzi, Jessica T. Davis, Marco Ajelli, et al. The effect of travel restrictions on the spread of the 2019 novel coronavirus (covid-19) outbreak. *Science*, 368(6489):395–400, 2020.
- [13] Cornelia Betsch, Lothar H. Wieler, and Katrine Habersaat. How behavioural science data helps mitigate the COVID-19 crisis. *Nature Human Behaviour*, 4(5):460–471, 2020.
- [14] Harald Schmidt, Lawrence O. Gostin, and David R. Williams. Is it lawful and ethical to prioritize racial minorities for covid-19 vaccines? JAMA, 324(20):2023–2024, 2020.